HEFAT2014
10th International Conference on Heat Transfer, Fluid Mechanics and Thermodynamics
14 – 16 July 2014
Orlando, Florida

USING AN ALL-SPEED ALGORITHM TO SIMULATE UNSTEADY FLOWS THROUGH MIXED HYDRO-PNEUMATIC SYSTEMS

Masoud Darbandi[1*], Amir A. Beige[1], MohammadAli Akbari[1] and Gerry E. Schneider[2]
[*]Author for Correspondence
[1]Center of Excellence in Aerospace Systems, Department of Aerospace Engineering,
Sharif University of Technology, P.O.Box 11365-8639, Tehran, Iran
[2]Department of Mechanical and Mechatronics Engineering, University of Waterloo,
Waterloo, ON, N2L 3G1, Canada
E-mail: darbandi@sharif.edu

ABSTRACT

In this paper, we take two important steps to analyse hydro-pneumatic systems and their components. In this regard, we first extend a new all-speed approach to solve the full one-dimensional Navier-Stokes equations. The extended approach can be equally used to simulate both gas and liquid flows, considering an equivalent gas constant for the latter case. We further apply the extended approach to analyse both liquid water and air flows through two separate hydro-pneumatic circuits. To verify the accuracy of our solution, we compare our solutions with those of Lax-Wendroff method. The comparison shows that the current proposed all-speed algorithm provides solutions with excellent accuracy. One important advantage of this new extended algorithm is in treating the two-phase fluid flow problems, where there are mixed liquid water and vapour behaviours, e.g., diaphragm pumps. Therefore, as a second contribution, we simulate a multi-component diaphragm pump, whose parts consist of check valves, signal subsystems, conveys, and air distribution system. As a final step, we obtain the limit of cavitation temperature at the suction side of the check valve for a sample diaphragm pump.

INTRODUCTION

High pressure hydro-pneumatic systems need to be constructed with high quality materials. These systems carry different flow rates and tolerate high pressures during their operations. To carry out careful simulations for such important systems, it is required to consider a multi-element framework with sufficient accuracies and capable of modeling the transient flow through very complex components at various gas/liquid flow conditions. Evidently, an efficient all-speed algorithm can predict the transient behavior of a hydro-pneumatic system without the need to apply for two individual or separate compressible and incompressible solvers and without the need to switch between them. It should be mentioned that the meaning of low-Mach number flow solution is totally different from the current all-speed algorithm, which solves pure incompressible flow in addition to different compressible flow cases using one unique algorithm.

Indeed, simulation of high pressure hydro-pneumatic systems is typically a difficult job because of the structural and functional complexities associated with such systems [1]. As an example, a diaphragm pump is a multi-component hydro-pneumatic system consisting of several simpler hydraulic and pneumatic parts, exhibiting unsteady behaviour due to its moving diaphragms. This system can be also subject to the risk for cavitation and a serious reduction in its life performance and endurance. As is known, the cavitation phenomenon can normally occur when the vapour pressure of the process fluid reaches the working chamber pressure. If this happens, the subsequent cavitation (e.g., wear, pressure shocks) would heavily reduce the pump's performance and lifetime. Since the numerical analysis of cavitation is often faced with crucial instabilities; due to using different numerical methods to achieve the interaction between two compressible and incompressible phases, the use of an all-speed method for both liquid and gas parts can greatly improve the multi-phase flow solution stability in treating complex hydro-pneumatic systems.

Simulating a diaphragm pump as a black box and without imposing the details of unsteady behaviour of its moving components would result in some disadvantages, e.g., ignoring some important mechanical behaviours like pressure pulsations, which can dramatically affect the correct modeling of a real diaphragm pump. Since we simulate a complete diaphragm pump, we can find the cavitation temperature limit for it and can consequently extend suitable instructions to avoid it. Additionally, by modeling a complete diaphragm pump, we would be readily able to take into consideration the unsteady behaviour of any hydro-pneumatic sub-components, which should be taken in modeling.

In this paper, we extend the simulation capabilities of an existing multi-element numerical framework and apply it to analyse a high pressure hydro-pneumatic circuit. In this regard, we first extend an all-speed flow solver capable of solving both liquid water and air flows through different hydro-pneumatic assemblies. Next, we compare the achieved solutions with those of Lax-Wendroff method. It should be noted that since the hydro-pneumatic systems deal with both gas and liquid phases simultaneously, the classical numerical methods can only be effective in solving certain flow regimes. However, an all-speed method, which can simultaneously solve both gas (compressible or incompressible) and liquid (incompressible) phases without any extra considerations, would help to achieve a more stable convergence procedure and reduce the solution time for the entire system. It is because we avoid switching between two compressible and incompressible solvers during the solution procedure. Eventually, we use our extended all-speed algorithm and simulate the flow behaviour through a real super-component diaphragm pump. Then, we show how we can avoid cavitation by specifying a working temperature limit for the suction side of the pump's check valve.

NOMENCLATURE

A	$[m^3]$	Pipe cross-sectional area
A_e	$[m^2]$	Effective area
C	[-]	Courant number
D	[m]	Pipe diameter
dx	[m]	Displacement of diaphragm middle point
dV	$[m^3]$	Volume change
e	$[m^2/s^2]$	Specific energy
F_w	$[\mathrm{kg}/(m^2 s^2)]$	Wall friction
k_1	[-]	Linearization constant
k_2	[-]	Linearization constant
p	$[\mathrm{kg}/(ms^2)]$	Pressure
P_w	[m]	Pipe perimeter
Pr	[-]	Prandtl number
Q_w	$[\mathrm{kg}/(ms^3)]$	Heat transfer from wall
Re	[-]	Reynolds number
t	[s]	Time
T_w	[K]	Wall temperature
u	[m/s]	Velocity
x	[m]	Position in pipe
Δt	[s]	Time step
Δx	[m]	Cell size
ε	[m]	Pipe roughness
λ	$[W/mK]$	Heat conductivity
λ_T	[-]	Turbulent friction factor
ρ	$[\mathrm{kg}/m^3]$	Density

SUBSCRIPTS-SUPERSCRIPTS-ACCENTS

e	[-]	east
o	[-]	old
w	[-]	Wall or west
overbar	[-]	Lagged from previous iteration

COMPUTATIONAL MODELING

The one-dimensional flow governing equations are given by

$$\frac{\partial \rho}{\partial t}+\frac{\partial(\rho u)}{\partial x}=0$$

$$\frac{\partial(\rho u)}{\partial t}+\frac{\partial(\rho u^2)}{\partial x}=-\frac{\partial p}{\partial x}-F_w \qquad (1)$$

$$\frac{\partial(\rho e)}{\partial t}+\frac{\partial(\rho u e+p u)}{\partial x}=Q_w$$

We choose the finite volume method to treat these equations. Darbandi and Schneider [2,3] developed an all-speed algorithm in which the discretized governing equations were simultaneously solved for pressure, temperature, and momentum component $(\equiv \rho u)$ variables. Comparing with the works of other investigators, who normally used the velocity component as the primary dependent variables in their algorithms, they showed that the use of momentum component $(\equiv \rho u)$ would result in several important advantages including a strong flow analogy creation between compressible and incompressible formulations. This enabled them to use any incompressible flow procedure to solve compressible flows [4]. Additionally, the momentum component would provide more simplification in linearization procedure [5], and a more effective suppression of oscillations for flows passing through discontinuities [2].

The finite volume treatment of flow equations would lead to

$$\begin{aligned}
&\frac{\Delta x(\rho_p-\rho_p^{\,0})}{\Delta t}+(\rho u)_e-(\rho u)_w=0\\
&\frac{\Delta x\left[(\rho u)_P-(\rho u)_P^0\right]}{\Delta t}+u_e(\rho u_e)-u_w(\rho u_w)+p_e-p_w=0\\
&\frac{\Delta x\left[(\rho E)_P-(\rho E)_P^0\right]}{\Delta t}+(\rho u e)_e-(\rho u e)_w+(p u)_e-(p u)_w=0
\end{aligned} \qquad (2)$$

in which the flow cross section area is taken unity.

Since the density variable is considered as a secondary unknown in our pressure-based algorithm, the transient term in the discretized continuity equation needs suitable linearization with respect to our chosen unknown variables. We employ a Taylor series expansion to consider active roles for both pressure and temperature terms as follows [3]:

$$\rho \approx \bar{\rho}+\frac{\overline{\partial \rho}}{\partial P}(P-\bar{P})+\frac{\overline{\partial \rho}}{\partial T}(T-\bar{T}) \qquad (3)$$

where

$$\frac{\overline{\partial \rho}}{\partial P}=\frac{1}{R\bar{T}} \qquad \frac{\overline{\partial \rho}}{\partial T}=-\frac{\bar{P}}{R\bar{T}^2} \qquad (4)$$

where the variables with an over bar indicate that they are approximated from the previous iteration.

In current method, the nonlinear convection terms are linearized with respect to the momentum component $(\equiv \rho u)$, which is a primary dependent variable in our algorithm. One sophisticated linearization scheme suggests [6]:

$$\rho uu \approx 2k_1\overline{u}(\rho u) - k_2\overline{u}^2\rho \tag{5}$$

where k_1 and k_2 are two arbitrary constants. If $k_1 = k_2 = 1$, it results in the Newton-Raphson linearization scheme as follows:

$$u(\rho u) \approx \overline{u}(\rho u) + (\overline{\rho u})u - \overline{\rho uu} \tag{6}$$

If $k_1 = 1$ and $k_2 = 0$, it would yield a simple linearization as follows:

$$\rho uu \approx \overline{u}(\rho u) \tag{7}$$

The flow variables are interpolated at the cell faces using the physical influence scheme (PIS), which utilizes the flow governing equations to derive the integration point expression. Using the PIS, the momentum component and temperature are derived at cell faces as follows:

$$(\rho u)_e = \frac{2C_e(A_P/A_e + \overline{\rho}_e/\overline{\rho}_P)}{1+4C_e}(\rho u)_P + \frac{C_e}{\overline{u}_e(1+4C_e)}(p_P - p_E) + \frac{(\rho u)_e^0}{1+4C_e} \tag{8}$$

$$T_e \approx \frac{2C_e}{1+2C_e}T_P + \frac{C_e\overline{p}_e}{(\overline{\rho u})_e c_v(1+2C_e)}\left(\frac{(\rho u)_P}{\overline{\rho}_P} - \frac{(\rho u)_E}{\overline{\rho}_E}\right) + \frac{(T)_e^0}{1+2C_e} \tag{9}$$

where the Courant number is defined as $C = \overline{u}\Delta t/\Delta x$ in this formulations. Also, the pressure term is linearly interpolated at the control volume cell faces.

Regarding the spatial accuracy, the current formulations perform second-order accurate in low Reynolds number flows. However, at very high Reynolds numbers, it reduces to a first-order scheme. Also, the current method is first-order accurate in time. It is worth to emphasize that the accuracy of the present numerical solution is excellent in spite of using a first-order scheme to treat high Reynolds number flows even on coarse grid distributions. It is because the use of inclusive cell-face expressions provides strong couplings between the pressure and velocity fields and minimizes the false diffusion in the domain [7].

Using the above described method of discretization, liquid incompressible flows can be simulated without adding any artificial compressibility. The detail algorithm for incompressible flow treatment has been shown in Figure 1. As is seen, the Jeffery and Austin [8] equation of state for liquid water is solved numerically in this process using the Newton-Raphson interpolation scheme. This provides the density as a function of pressure and temperature. This equation of state would be much more accurate than an equivalent simple cubic equations of state over wide ranges of pressure (0.1-3000 bar) and temperature (-34-1200 °C) fields, which are typically encountered in hydro-pneumatic systems. The derived value of density is inserted in the ideal gas equation (see Figure 1) to find equivalent gas constant for liquid water condition. Although this constant is not realistic, it is considered in our formulations to simulate liquid water flow in the same way as for gases. Indeed, the computation time for solving the liquid water EOS to obtain an equivalent gas constant is small comparing with the total time required to solve the linear algebraic system of equations.

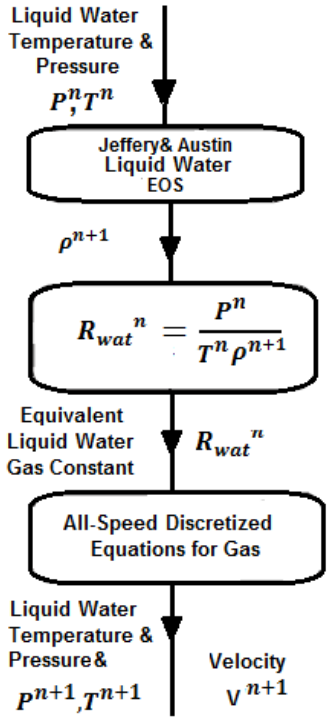

Figure 1 The procedure to solve liquid water flow using the current all-speed algorithm

The friction losses are considered in the current formulations using the Zigrang-Sylvester friction factor estimation. It is given by

$$F_w = \lambda_T \rho V^2/(2d) \tag{10}$$

where

$$\frac{1}{\sqrt{\lambda_T}} = -2\log_{10}\left\{\frac{\varepsilon/D}{3.7} + \frac{2.51}{\mathrm{Re}}[1.14 - 2\log_{10}(\frac{\varepsilon}{D} - \frac{21.25}{\mathrm{Re}^{0.9}})]\right\} \tag{11}$$

We also use some specific relations to compute the convection heat transfer coefficient and the corresponding heat transfer from the walls using [9]:

$$h = 0.023\ \mathrm{Re}^{0.8}\mathrm{Pr}^{0.33}\lambda/\mathrm{d} \tag{12}$$

$$Q_w = hP(T_w - T)/A \tag{13}$$

A double diaphragm pump as a super-component system is modeled in this paper. It is consisted of four parts of diaphragm, signal system, conveys, and check valves. Figure 2 presents a schematic representation of the current chosen double diaphragm pump. To model the mechanical aspects of this pump, it is assumed that no net mechanical force is exerted on the diaphragms and that the diaphragm motion is described through an effective area following specific relations between the volume change and the diaphragm middle point displacement. This relation is given by

$$dV = A_e(x)\, dx \tag{14}$$

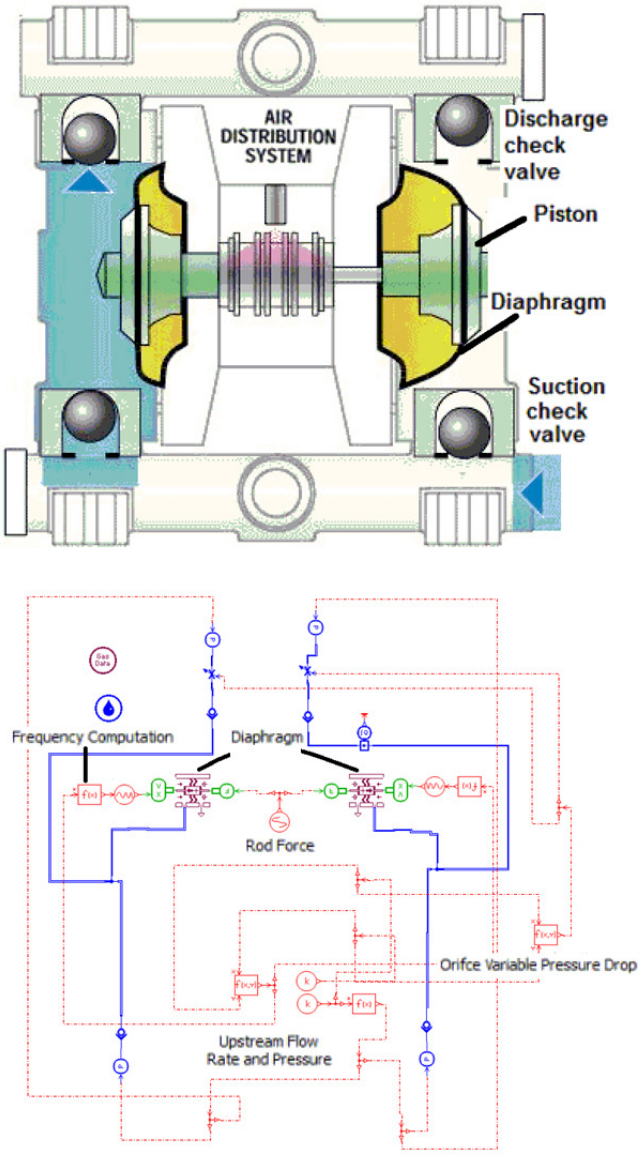

Figure 2 Schematic of the investigated double diaphragm pump and its equivalent hydro-pneumatic circuit

The effective area can be estimated either using experimental observation or the finite element modeling of the flow through the diaphragm pump considering the diaphragm structure interaction. The effective diameter corresponding to the effective area is assumed to be constant (11 cm) in this work. It is also obvious from the pump performance maps (e.g., see Figure 3) that the pump outlet pressure would be a function of air distribution system flow variables. In order to simulate this behaviour, variable loss orifices are added to the double diaphragm pump model to simulate pressure drop in a way that it is consistent with its real behaviour.

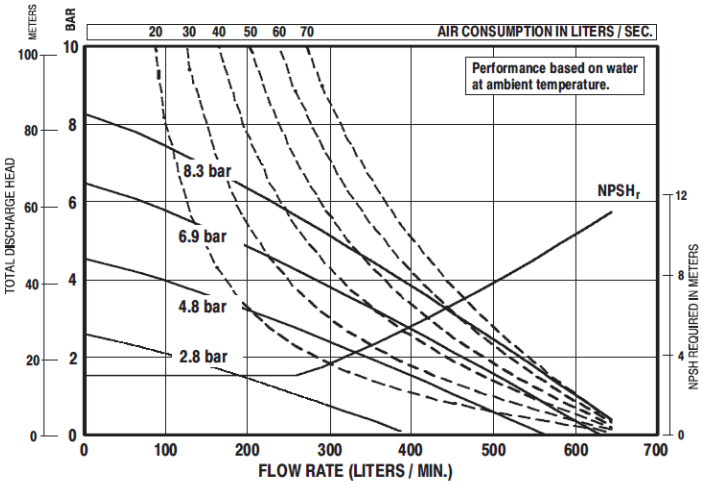

Figure 3 Performance map for the simulated double diaphragm pump [10]

To model the unsteady characteristics of the simulated pump, the frequency of diaphragm motion is computed assuming that the swept volume per stroke does not change during the pump operation. So, the pump frequency is a linear function of its flow rate in our modeling.

RESULTS AND DISCUSSION

Two test cases are considered to evaluate the current method in treating both gas and liquid flows. A schematic of the investigated air (pneumatic) system is shown in Figure 4. Source 1, S1, charges a $4m^3$ chamber, i.e., C1, to a pressure of 200 Bars. The velocity and pressure magnitudes are computed along pipe P1 using the described all-speed finite-volume algorithm. The velocity and pressures have been plotted along pipe length P1 in Figures 5 and 6, respectively. We have also used the second-order Lax-Wendroff method to verify the current solutions [11,12]. The comparisons show that the current method has been accurate enough to present reliable solution in this test case. This is where we have not applied any artificial numerical damping into our algorithm. This is where the second-order Lax-Wendroff method needed such side considerations. Our experience showed that using different friction calculations and different discretization types would lead to some discrepancies in our results.

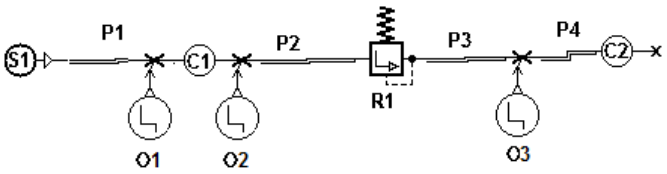

Figure 4 Schematic of the investigated pneumatic system

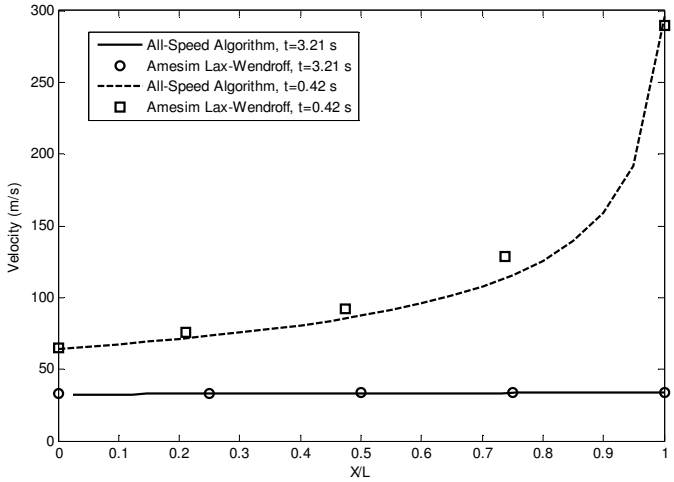

Figure 5 Velocity distribution in a gas line and comparison with that of the Lax-Wendroff method at two different time levels

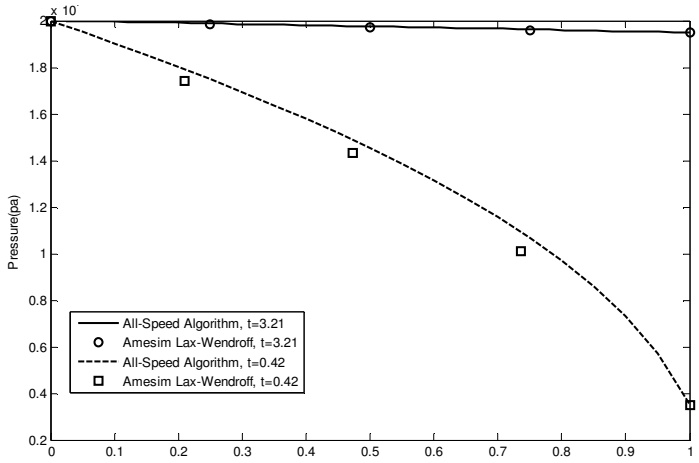

Figure 6 Pressure distributions in a gas line and comparison with that of the Lax-Wendroff method at two different time levels

Figure 7 verifies that the current algorithm fully conserves the mass flow through circuit P1. We can achieve a more accurate mass conservation results by increasing the number of grid nodes from 21 to 41; however, the finite difference Lax-Wendroff method does not show any change in its mass flow distribution with more grid refinements.

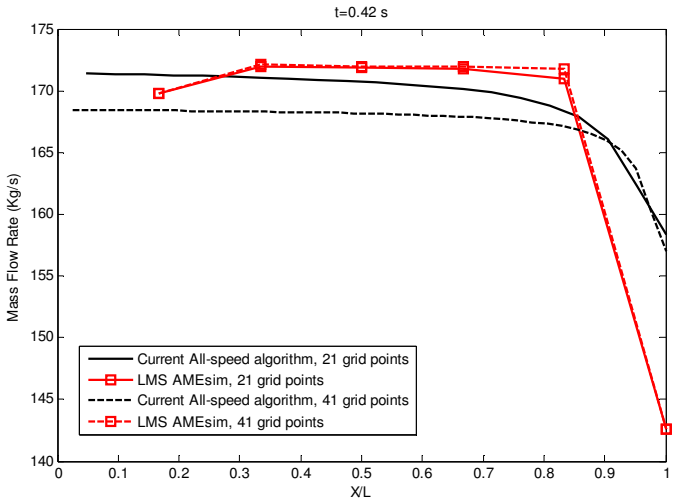

Figure 7 Evaluating the mass conservation through pneumatic line using the current method and that of a commercial software

The second test case is to simulate the liquid water flow through a pipe with an inflow pressure of 87.1 Bars, a temperature of 280 K, and imposing different outlet pressure magnitudes. Figure 8 shows the velocity distribution along this pipe considering different pressure outlet conditions. The current results are compared with the solutions derived from the LMS Amesim software. The agreement between them is excellent.

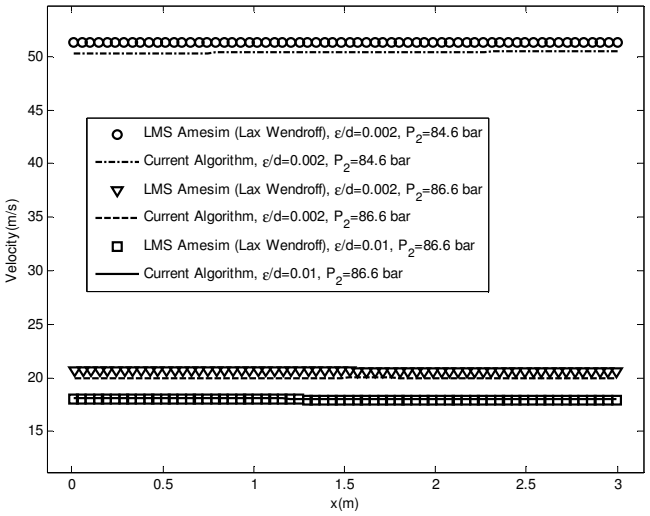

Figure 8 Velocity distributions in a liquid line and comparison with that of the Lax-Wendroff method

Figures 9 and 10 present the results for a simulated double diaphragm pump including its outlet pressure and the volume flow rate with time, respectively. The results presented in these figures were obtained for air pressure of 6.9 bars and an air flow rate of 40 l/sec. As is seen in this figure, there are some oscillations near the mean value found in the pump manufacturer performance map (see Figure 3) for the specified air flow rate and pressure.

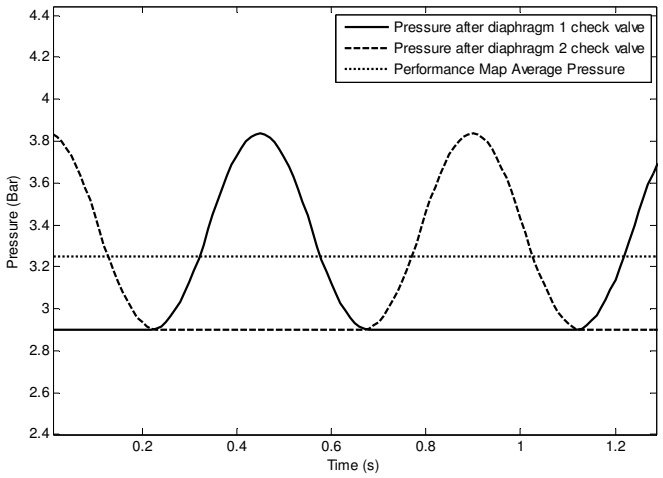

Figure 9 Variation of the simulated diaphragm pump outlet pressure with respect to time and comparison with the pump performance map data

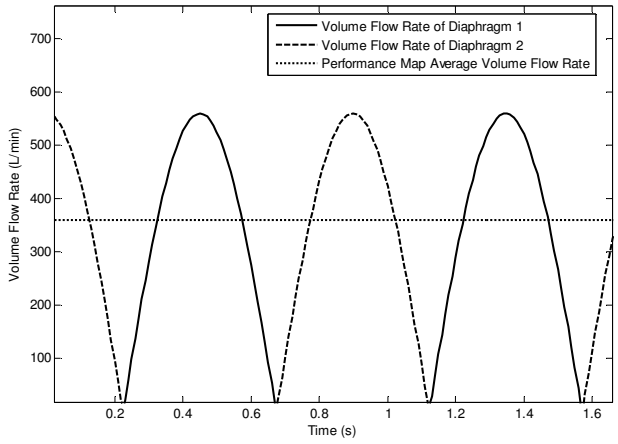

Figure 10 Variation of the simulated diaphragm pump volume flow rate with respect to time and comparison with the pump performance map data

As is known, the check valves of diaphragm pumps are subject to different pressure magnitudes during their pumping cycles. This can lead to a cavitation appearance inside the pump. The phase change from liquid to gas can harm the pump [13]. In this work, we predict the fluid thermodynamic properties, which can be used to specify the cavitation point at downstream of the suction valve. Figure 11 illustrates the time history of pressure variation behind the pump suction check valve. Inspecting this figure, it is obvious that the pump would experience the cavitation condition, if the inflow temperature exceeds 80 ^{o}C. That is because the valve local pressure would reduce under the saturation vapour pressure at the achieved temperature.

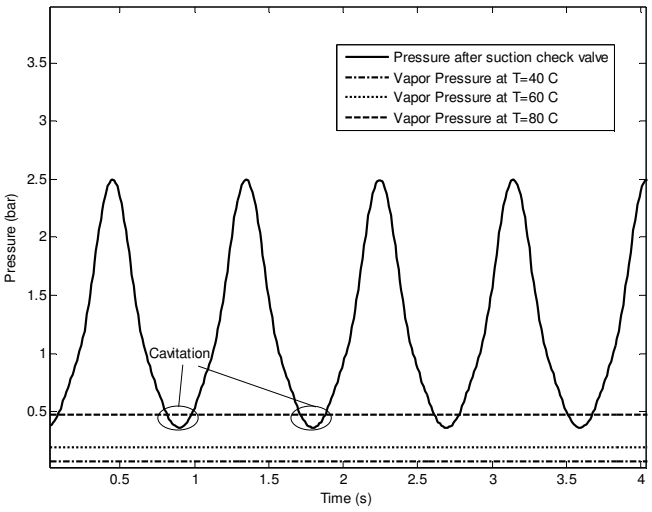

Figure 11 Calculating the cavitation temperature limit at the suction check valve of the simulated diaphragm pump

CONCLUSION

We developed an all-speed algorithm to treat two-phase flows through mixed hydraulic-pneumatic systems. The formulation was extended for solving the one-dimensional full Navier-Stokes equations. As was expected, the extended method and formulation would be able to treat both liquid and gas flows as well as mixed two-phase flows. To prove this, we used this method and solved a number of test cases including a diaphragm pump. This method helped us to take into consideration all moving parts in the diaphragm pump assembly in our simulation. Therefore, we could model the diaphragm pump and its subcomponents at different diaphragm pump operating conditions. Our numerical results showed that it was possible to model both air and water phases in the same way. Indeed, the current numerical method can help to analyse the hydro-pneumatic systems without the need to apply for two different compressible and incompressible solvers. The use of two different solvers can lead to inappropriate convergences during the fluid flow solutions. The current results showed that the extended finite-volume method would perform better mass conservation in comparison with the Lax-Wendroff finite-difference method. We used our extended solver and simulated a diaphragm pump. We were able to predict the cavitation condition limit for this pump using thermodynamic variables. In future, we will be able to predict the cavitation behaviour by covering gas-liquid interactions, using the current extended finite-volume method.

ACKNOWLEDGMENTS

The authors would like to acknowledge the grant received from the Deputy of Research and Technology in Sharif University of Technology. This financial help is highly acknowledged and appreciated.

REFERENCES

[1] Mobley R. K., Fluid Power Dynamics, Newnes, 2000.

[2] Darbandi M. and Bostandoost S.M., A new formulation toward unifying the velocity role in collocated variable arrangement, *Numerical Heat Transfer* B 47, 2005, pp. 361–382.
[3] Darbandi M. and Schneider G.E., Analogy-based method for solving compressible and incompressible flows, *Journal of Thermophysics and heat Transfer,* Vol.12, 1998, pp. 239–247.
[4] Darbandi M. and Hosseinizadeh S.F., General pressure-correction strategy to include density variation in incompressible algorithms, *Journal of Thermophysics and Heat Transfer,* Vol.17, 2003, pp. 372-380.
[5] Darbandi M. and Schneider G.E., Comparison of pressure-based velocity and momentum procedures for shock tube problem, *Numerical Heat Transfer, Part B* 33, 1998, pp. 287-300.
[6] Darbandi M., Roohi E., and Mokarizadeh V., Conceptual Linearization of Euler Governing Equations to Solve High Speed Compressible Flow Using a Pressure-Based Method, *Numerical Methods for Partial Differential Equations*, Vol. 24, No. 2, 2008, pp.583-604.
[7] Darbandi M. and Vakilipour S., Developing implicit pressure-weighted upwinding scheme to calculate steady and unsteady flows on unstructured grids, *International Journal for Numerical Methods in Fluids*, Vol.56, 2008, pp. 115-141.
[8] Jeffery C.A., Austin P.H., A new analytic equation of state for liquid water, *J. Chem. Phys.*, 1999,110 (1) pp. 484–496.
[9] INEL, 2001, RELAP5/MOD3 Code Manual, Models and Correlations NUREG/CR-5535, Rev1-Vol, vol. IV.
[10] ARO pump performance curves, Ingersoll Rand Company Ltd, 2010.
[11] Scavarda S., and Bideaux E., A Pneumatic Library for AMESim, Proceedings of ASME International Mechanical Engineering Conference and Exhibition, IMECE'98 Anaheim, California, Nov. 1998 pp.197-206.
[12] LMS Amesim Hydraulic Library Manual, LMS Imagine.lab, 2010.
[13] Vetter G., Depmeier L., and Schubert W., Design and Installation Conditions of Diaphragm Pumps for High-Pressure and Supercritical Fluids, *The Journal of Supercritical Fluids*, Vol. 5,1992,pp. 180-185.